# Supporting Information

# Highly Planarized Naphthalene Diimide-Bifuran Copolymers with Unexpected Charge Transport Performance

Rukiya Matsidik,[†,∥] Alessandro Luzio,[‡] Özge Askin, [‡] Daniele Fazzi,[§] Alessandro Sepe,[◊] Ullrich Steiner, [◊] Hartmut Komber,[⊥] Mario Caironi,[‡,*] and Michael Sommer [†,∥,#,○*]

[†] Universität Freiburg, Institut für Makromolekulare Chemie, Stefan-Meier-Str. 31, 79104 Freiburg, Germany

[∥]Freiburger Materialforschungszentrum, Stefan-Meier-Str. 21, 79104 Freiburg, Germany

[‡] Center for Nano Science and Technology @PoliMi, Istituto Italiano di Tecnologia, Via Pascoli 70/3, 20133, Milano, Italy

[§] Max-Planck-Institut für Kohlenforschung (MPI-KOFO), Kaiser-Wilhelm-Platz 1, D-45470, Mülheim an der Ruhr, Germany

[◊] Adolphe Merkle Institute, University of Fribourg, Chemin des Verdiers 4, CH-1700, Fribourg, Switzerland

[⊥] Leibniz Institut für Polymerforschung Dresden e.V., Hohe Straße 6, 01069 Dresden, Germany

[#] FIT Freiburger Zentrum für interaktive Werkstoffe und bioinspirierte Technologien, Georges-Köhler-Allee 105, 79110 Freiburg, Germany

[○] present address: Technische Universität Chemnitz, Polymerchemie, Straße der Nationen 62, 09111 Chemnitz.

## 1. Synthesis and Instrumentation

### 1.1. Synthesis

All materials used are purchased from Sigma Aldrich and used without further treatment unless otherwise stated. THF was purchased from Sigma Aldrich and dried over potassium under argon atmosphere. 2,6-Dibromonaphthalene-1,4,5,8-tetracarboxylic-N,N-bis(2-octyldodecyl)diimide,[1] 2,6-bis(2-bromothien -5-yl)naphthalene-1,4,5,8-tetracarboxylic-N,N-bis(2-hexyldecyl)diimide,[1] 2,6-bis(2-bromothien-5-yl) naphthalene-1,4,5,8-tetracarboxylic-N,N-bis(2-decyldodecyl)diimide,[1] and active Rieke zinc[2] were prepared according to previously reported methods.

**BrFuNDIFuBr**:

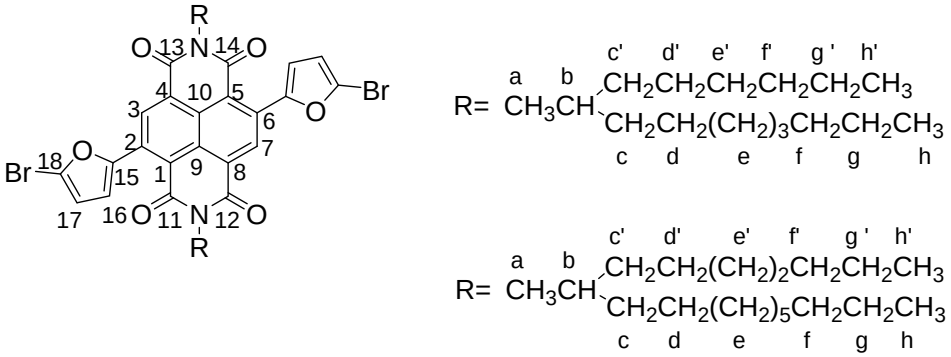


Under $N_2$ atmosphere, to a $CHCl_3$ solution (0.023 M) of FuNDIFu-C16 (91 mg, 0.107 mmol), N-bromosuccinimide (NBS) (39.16 mg, 0.22 mmol) was added. Then the mixture was stirred for 40 hours at room temperature (controlled by thin-layer chromatography). $CHCl_3$ was removed prior to recrystallization in ethanol (150 mL) to give 95 mg of a deep red solid in 85 % yield. FuNDIFu-C20 was brominated utilizing the same method; reaction yield is 92 %.

*2,6-Bis(2-bromofuran-5-yl)naphthalene-1,4,5,8-tetracarboxylic-N,N-bis(2-hexyldecyl)diimide* (BrFuNDIFuBr-C16): $^1$H NMR (300 MHz, $CDCl_3$): 9.03 (s, 2H, $H_{3/7}$), 7.35(d, J = 3.6 Hz, 2H, $H_{17}$), 6.59 (d, J = 3.6 Hz, 2H, $H_{16}$), 4.14 (d, J = 7.3, 4H, $H_a$), 1.98 (m, 2H, $H_b$), 1.5-1.1(48 H, $H_{c\text{-}g,\ c'\text{-}g'}$), 0.85 ppm

(12H, $H_{h,h'}$). $^{13}C$ (75 MHz, $CDCl_3$): 162.52 ($C_{12/14}$), 162.49 ($C_{11/13}$), 152.44 ($C_{15}$), 133.69 ($C_{2/6}$), 133.29 ($C_{3/7}$), 127.25($C_{17}$), 125.89 ($C_{16}$), 125.34 ($C_{9/10}$), 120.68 ($C_{4/8}$), 117.78 ($C_{1/5}$), 112.4 ($C_{18}$), 45.13 ($C_a$), 36.59 ($C_b$), 31.90 and 31.89 ($C_{f, f'}$), 31.75 and 31.71 ($C_{c,c'}$), 30.01−29.32 ($C_{e\ e'}$), 26.50 ($C_{d,d'}$), 22.67 ($C_{g,g'}$), 14.12 ($C_{h,h'}$) .

*2,6-Bis(2-bromofuran-5-yl)naphthalene-1,4,5,8-tetracarboxylic-N,N-bis(2-octyldodecyl)diimide* (BrFuNDIFuBr-C20): $^1H$ NMR (300 MHz, $CDCl_3$): 9.03 (s, 2H, $H_{3/7}$), 7.35(d, J = 3.6 Hz, 2H, $H_{17}$), 6.59 (d, J = 3.6 Hz, 2H, $H_{16}$), 4.14 (d, J = 7.3, 4H, $H_a$), 1.98 (m, 2H, $H_b$), 1.5-1.1(64 H, $H_{c\text{-}g,c'\text{-}g'}$), 0.85 ppm (12H, $H_{h,h}$). $^{13}C$ (75 MHz, $CDCl_3$): 162.52 ($C_{12/14}$), 162.49 ($C_{11/13}$), 152.44 ($C_{15}$), 133.69 ($C_{2/6}$), 133.29 ($C_{3/7}$), 127.25($C_{17}$), 125.89 ($C_{16}$), 125.34 ($C_{9/10}$), 120.68 ($C_{4/8}$), 117.78 ($C_{1/5}$), 112.4 ($C_{18}$), 45.13 ($C_a$), 36.58 ($C_b$), 31.93 and 31.91 ($C_{f,f'}$), 31.74 ($C_{c,c'}$), 30.04 −29.32 ($C_{e,e'}$), 26.53 ($C_{d,d'}$), 22.70 and 22.69 ($C_{g,g'}$), 14.14 ($C_{h,h'}$) .

**PNDIFu2-C16**:

Under argon atmosphere, to a dry THF solution (0.02 M) of BrFuNDIFuBr-C16 (221.09 mg, 0.22 mmol) in a one-neck round bottom flask, 0.33 mmol freshly made Rieke zinc in THF (2.46 mL) was added dropwise while stirring at room temperature. The color of the mixture immediately changed to deep green from previous red upon adding the active Rieke zinc suspension indicating the formation of radical anion, the mixture then was further stirred for one hour at RT to complete reaction. Then the radical anion (found to be extremely sensitive to $O_2$ and water) was carefully transferred to another round bottom flask equipped with a septum and $NidpppCl_2$ (11.93 mg, 0.022 mmol) through a syringe filter (0.45 μm). The whole mixture was placed to a preheated oil bath (50 °C) and stirred for 3 h. After cooling to RT the polymer solution (precipitated polymers were dissolved in $CHCl_3$) was precipitated into methanol (250 mL). The precipitate was filtered and purified with soxhlet extraction using acetone, ethylacetate and iso-hexanes before collecting with $CHCl_3$. Finally, the $CHCl_3$ polymer solution, deep

green in color, was filtered through a silica plug and concentrated and dried to give 167 mg dark black solid. SEC ($CHCl_3$ at room temperature): $M_n/M_w$ = 16.0 /38.1 kDa.

### 1.2. Instrumentation

*SEC measurements* were carried out on four SDV gel 5 µm columns, with pore sizes ranging from 103 to 106 Å (PSS), connected in series with a Knauer K-2301 RI detector, and calibrated with polystyrene standards. CHCl3 was used as eluent at room temperature at a flow rate of 1.0 mL/min.

*UV-vis measurements* were carried out on a Shimadzu 1800 spectrophotometer, using a tungsten lamp as the excitation source.

*DSC measurements* were acquired on a NETZSCH DSC 204 F1 Phoenix under a nitrogen atmosphere at a heating and cooling rate of 10 K $min^{-1}$.

*Thermogravimetric analysis* (TGA) was carried out on a Perkin TGA 4000 between 50−650 °C at 10 K $min^{-1}$under nitrogen.

*NMR spectroscopy.* $^1H$ NMR spectra were recorded on a Bruker Avance II 300 MHz and on a Bruker Avance III 500 MHz spectrometer. $CDCl_3$ was used as solvent for the monomers. High-temperature 500 MHz $^1H$ NMR spectra of the polymers were obtained from $C_2D_2Cl_4$ solutions. The solvents were used as chemical shift reference ($CDCl_3$: $\delta(^1H)$ = 7.26 ppm; $C_2D_2Cl_4$: $\delta(^1H)$ = 5.98 ppm).

*CV measurements* were carried out using a standard commercial electrochemical analyzer with a three-electrode single-compartment cell under nitrogen atmosphere. The working electrode was a silver coated glass, the counter electrode was a Platinum plate with same surface area as working electrode, and the operating reference electrode was an Ag/Ag wire (SCE). All the measurements were performed in

0.1 M $TBAPF_6$ (tetrabutylammonium hexafluorophosphate) solution of acetonitrile at room temperature and ferrocene is used as external standard.

*Grazing Incidence Wide-Angle X-Ray Scattering (GIWAXS).* Part of the in-situ GIWAXS measurements were carried-out at the beamline D1, Cornell High Energy Synchrotron Source (CHESS), Cornell University, Ithaca, NY, U.S.A. The wavelength was $\lambda = 1.15$ Å. The beam was focused to a size of 500 μm × 100 μm (horizontal × vertical) at the sample position. A beam stop for the primary beam and the small-angle X-ray scattering signal was employed. A CCD detector with a pixel size of 46.9 μm × 46.9 μm was used for GIWAXS with a sample− detector distance of 0.11 m. In order to choose the appropriate incident angle, an X-ray reflectometry scan was performed before recording the image. Part of the GIWAXS measurements were performed at the Adolphe Merkle Institute beamline under vacuum (University of Fribourg, Switzerland). The scatterless beamline employed the high brilliance Rigaku MicroMax-007HF, equipped with a rotating Cu-anode. The beam was focused to a size of 500 μm2 at the sample position, with a footprint on the sample averaging over circa 1 cm length. A beam stop for the primary beam, specularly reflected beam and diffuse scattering along the $q_y = 0$ was employed. An image plate was used for GIWAXS with a Sample-to-Detector Distance (SDD) of 0.1 m. For both synchrotron and laboratory measurements, images were then taken at an incident angle ($\alpha_i$) which is slightly higher than the critical angle of the film ($\alpha_{cf}$) and lower than the critical angle of the substrate ($\alpha_{cs}$). Thus, the entire film was penetrated, the internal film structures could be detected and the beam was fully reflected from the sample/substrate interface. Furthermore, at these incident angles the beam footprint on the sample is similar to the whole sample size. The samples were moved out of the beam after each measurement to avoid beam damage. The entire film thickness was

thus investigated, the thin films were methodically probed and any change occurring to their internal structures could be detected. The $q$-space calibration was performed fitting the characteristic scattering signal arising from silver behenate. The conversion of the 2D images from pixels to $q$-values as well as

the analysis of the 2D scattering maps were carried out using Xi-CAM (http://www.camera.lbl.gov/#!xi-caminterface/z8vcm).

*FET fabrication.* FETs with channel width of 2 mm and channel length of 20 μm were fabricated using a top-gate, bottom-contact geometry. Bottom Au contacts were defined by a lift off photolithographic process on glass (Corning Glass 1737F purchased from Apex Optical Services) with a 0.7 nm thick Cr adhesion layer. The thickness of the Au contacts was 15 nm. Solutions of PNDIT2-C16, PNDIT2-C20, PNDIFu2-C16, PNDIFu2-C20 in various solvents (5-9 g/L) were deposited by regular spin-coating at 1000 rpm for 60 s in air. The semiconductor was then annealed for 30 min at different temperature, ranging from 100 °C to 300 °C on a hot plate in a nitrogen atmosphere. PMMA (Sigma-Aldrich) with $M_w$ = 120 kDa was spun from n-butyl acetate (with a concentration of 80 g/L), resulting in 550 nm thick dielectric layer (ε = 3.6). Al electrodes were thermally evaporated as gate contacts. The electrical characteristics of transistors were measured in a nitrogen glove box on a Wentworth Laboratories probe station with an Agilent B1500A semiconductor device analyzer. Linear and saturation charge carrier mobility values were extracted according to gradual channel approximation.

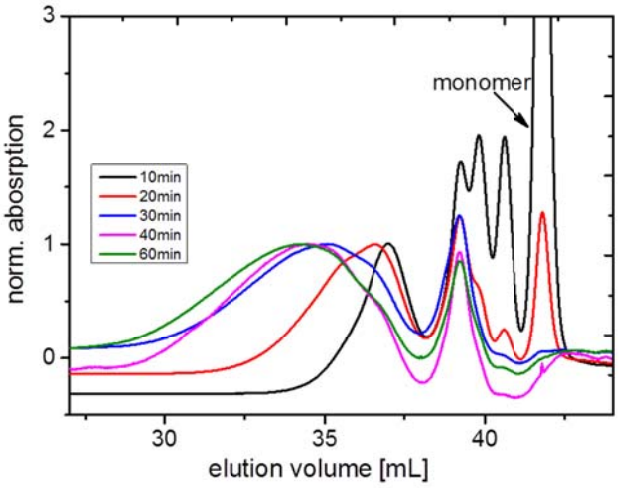


**Figure S1**. SEC curves of aliquots taken during polymerization (PNDIFu2-C16) in $CHCl_3$ at room temperature.

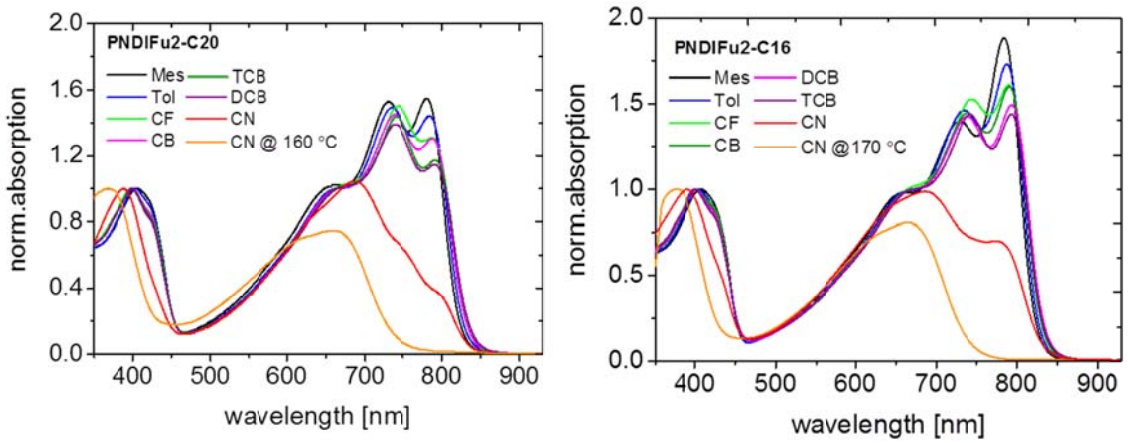


**Figure S2**. UV-vis absorption spectra of PNDIFu2-C20 and -C16 in various solvents at room temperature

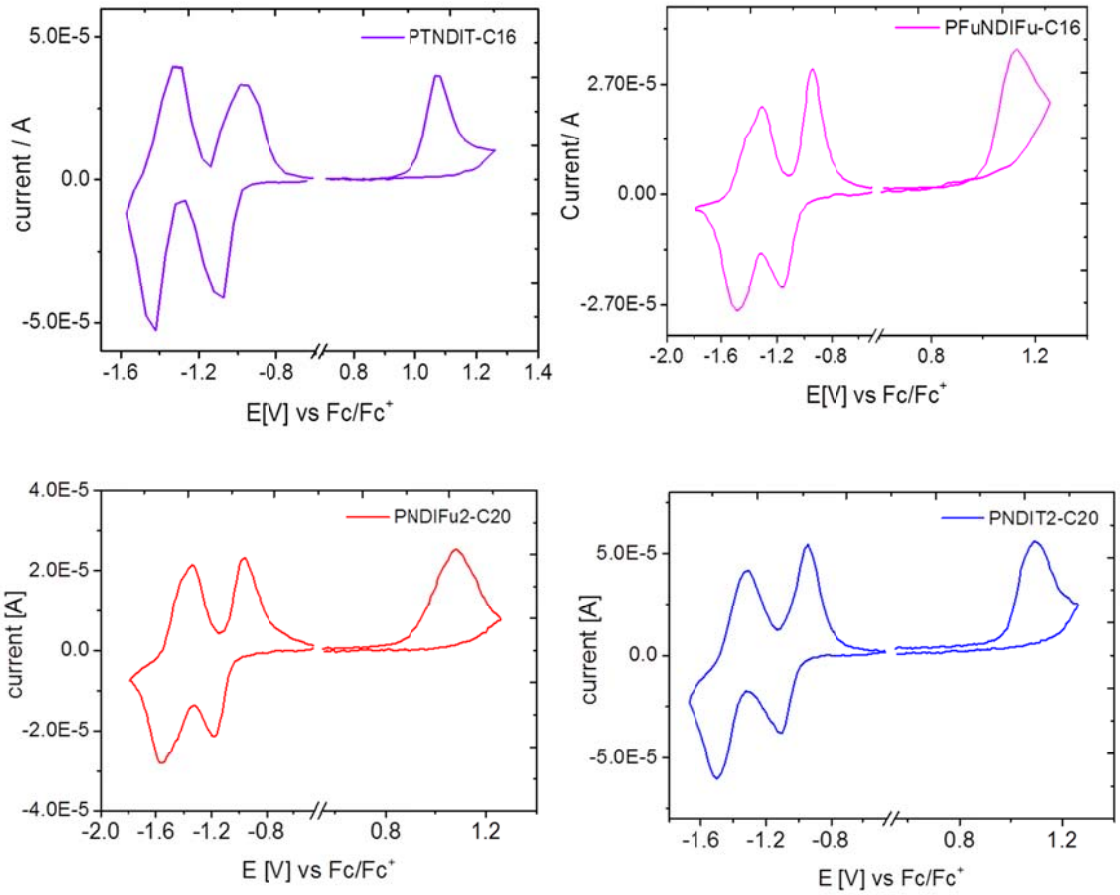


**Figure S3**. Representative cyclic voltammetry curve of polymer films in 0.1 M $TBAPF_6$ acetonitrile solution at a 50 mV/s scan rate.

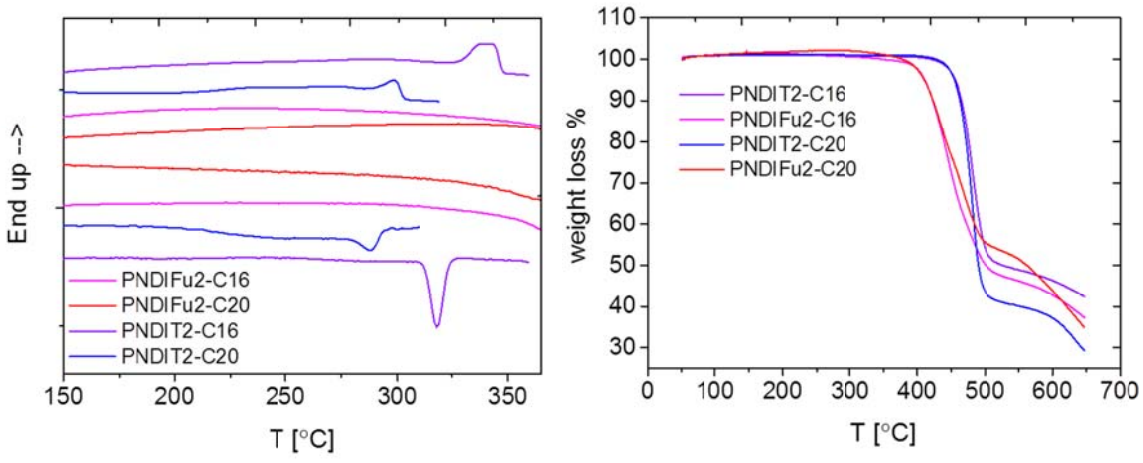


**Figure S4.** DSC and TGA curves of all four copolymers measured at 10 K/min under $N_2$.

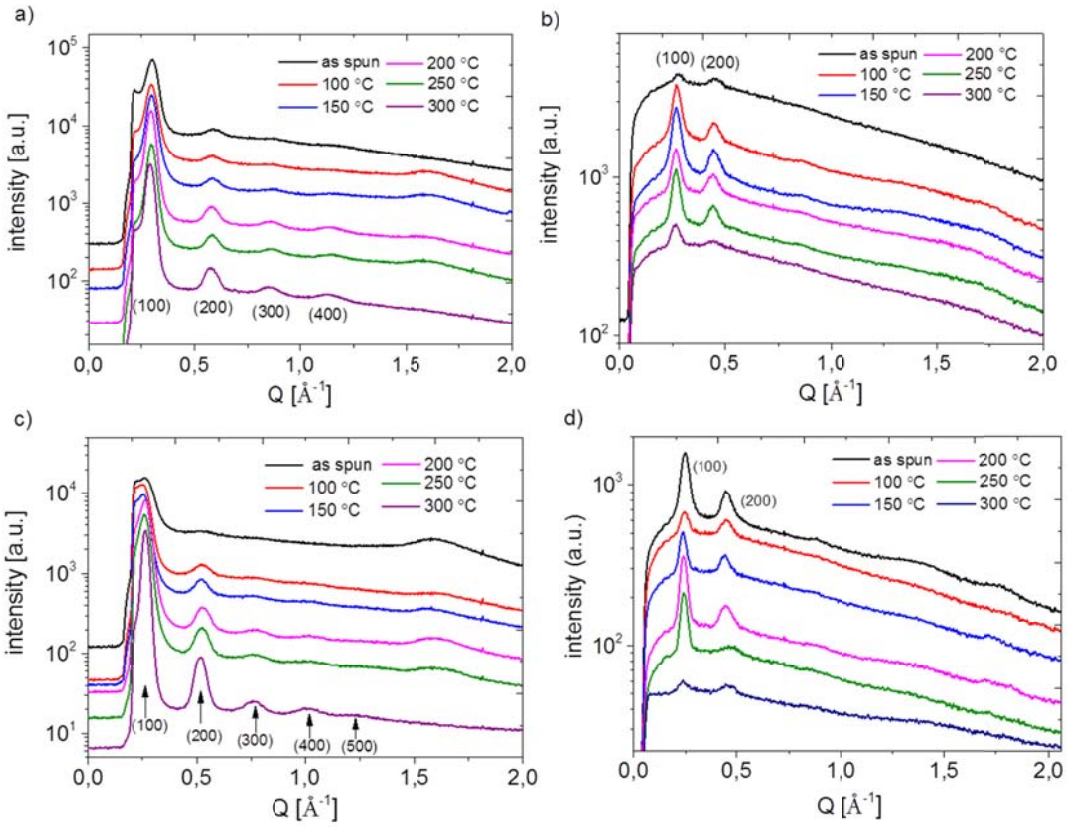


**Figure S5.** 1D GIWAXS scattering profiles of PNDIT2-C16 (a, b) and PNDIT2-C20 (c, d) films annealed at different temperatures: vertical (a, c) and horizontal (b, d) integrations

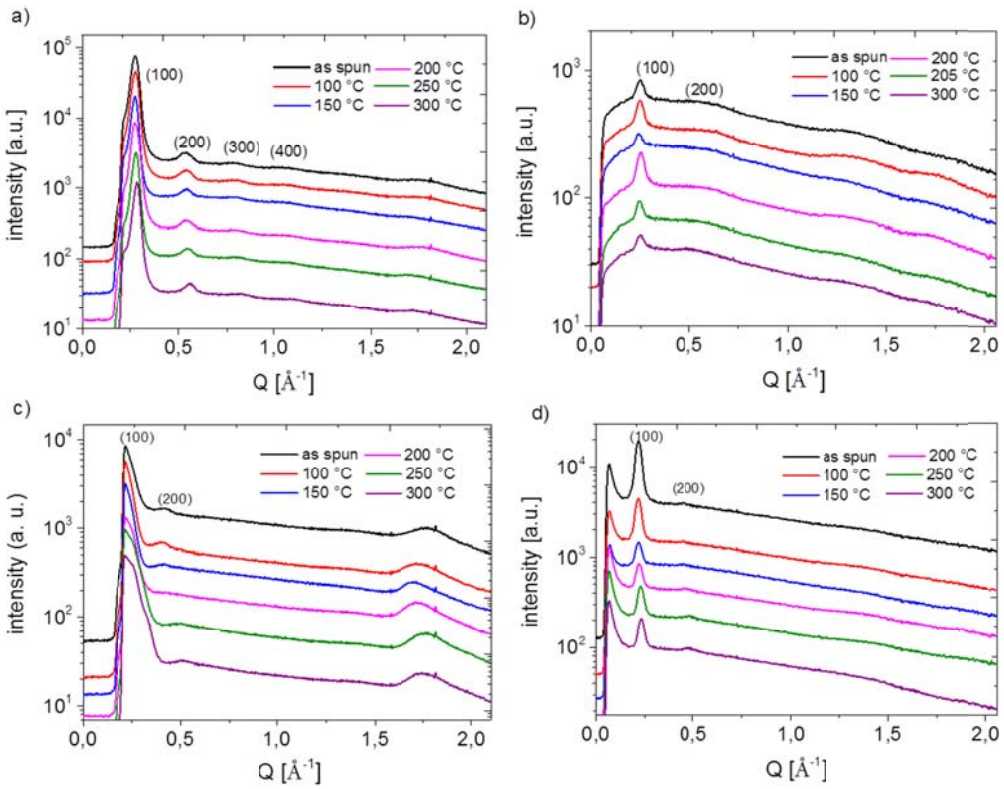


**Figure S6.** 1D GIWAXS scattering profiles of PNDIFu2-C16 (a, b) and PNDIFu2-C20 (c, d) films annealed at different temperatures: vertical (a, c) and horizontal (b, d) integrations

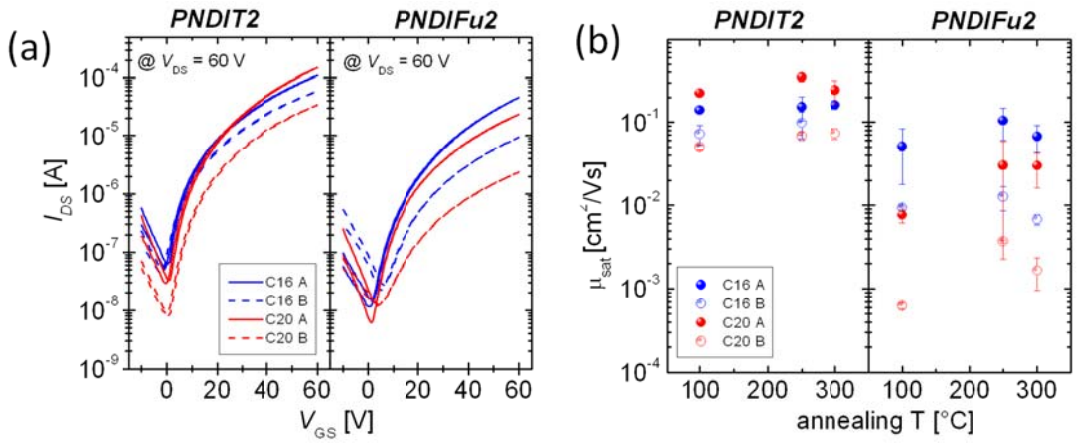


**Figure S7.** (a) Transfer characteristics of FETs with films deposited from DCB exemplary annealed at 250 °C (b) plot of mean saturation mobility values ($\mu_{sat}$) versus thermal annealing temperature on semiconductor films.

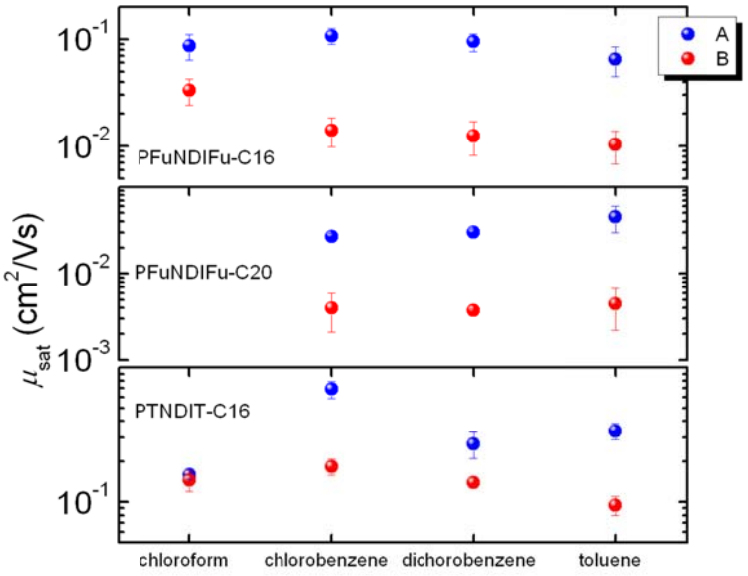


**Figure S8.** Plot of mean saturation mobility values ($\mu_{sat}$) versus the processing solvent. Before dielectric deposition PNDIT2 and PNDIFu2 films underwent thermal annealing of 120 °C. Investigation of solvent effect for PNDIT2-C20 has been reported elsewhere[19].

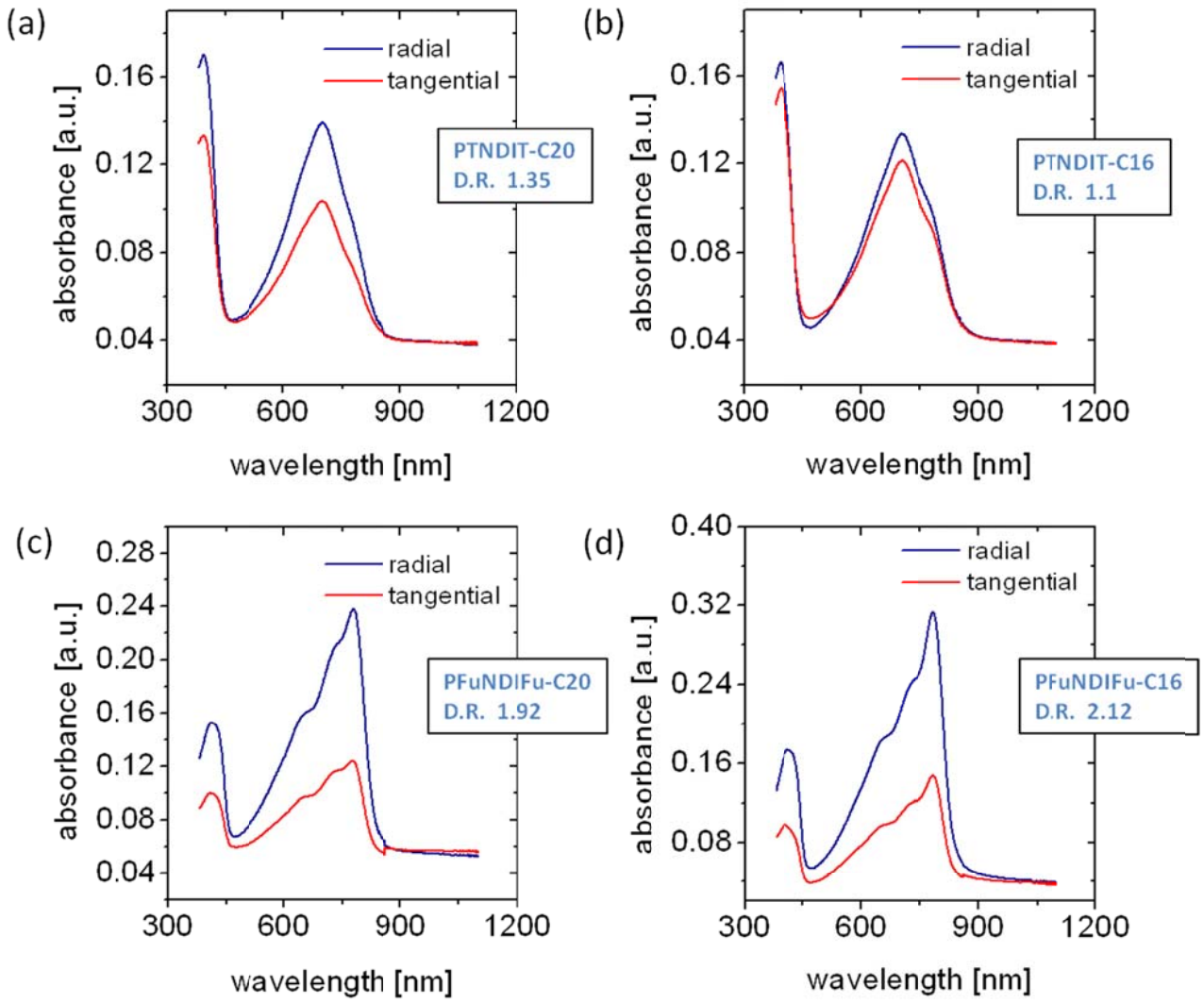


**Figure S9.** Polarized UV-vis absorption spectra of films aligned using best solvent formulation and off-centre spin-coating deposition method; Optical dichroic ratios (D.R.) are also reported.

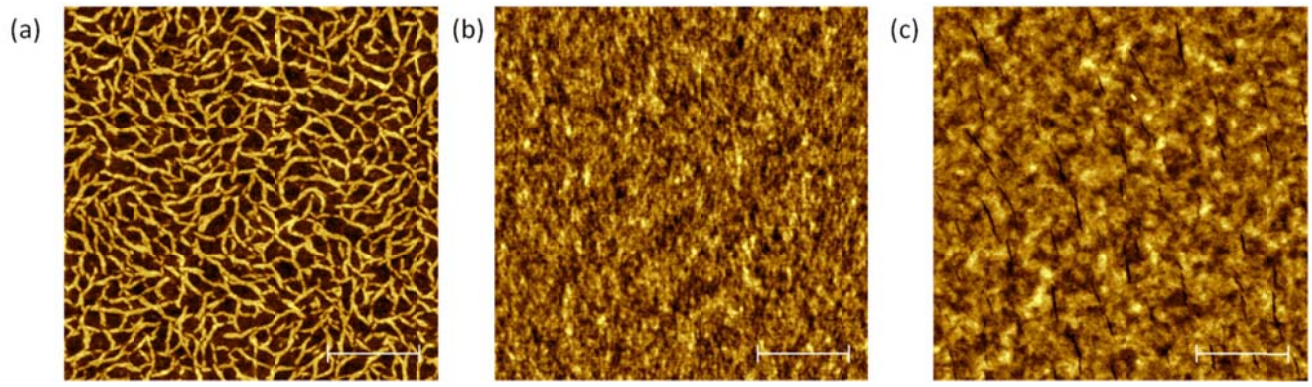


**Figure S10.** Atomic force microscopy (AFM) height images of PNDIT2-C20 films spin coated from toluene at a concentration of 0.2 g/l solution (a), 5 g/L (as spun) (b) and 5 g/L (after 30 minutes thermal treatment at 250 °C) (c); dilute solution (a) results in fibrillar networked monomolecular (2.5 nm thick) layer, as expected. Bulky films annealed at low temperature (b) display typical fibrillar-like morphology with elongated domains mostly aligned along the flow direction (root mean roughness $R_{rms}$ = 0.4 nm); high temperature annealing results in a loss of fibrillar microstructure, the occurring of fractures mostly along the flow direction and a slightly increased roughness ($R_{rms}$ = 0.56 nm), as a consequence of the strong film morphological rearrangement also observed by GIWAXS. In all images, scale bars are 500 nm.

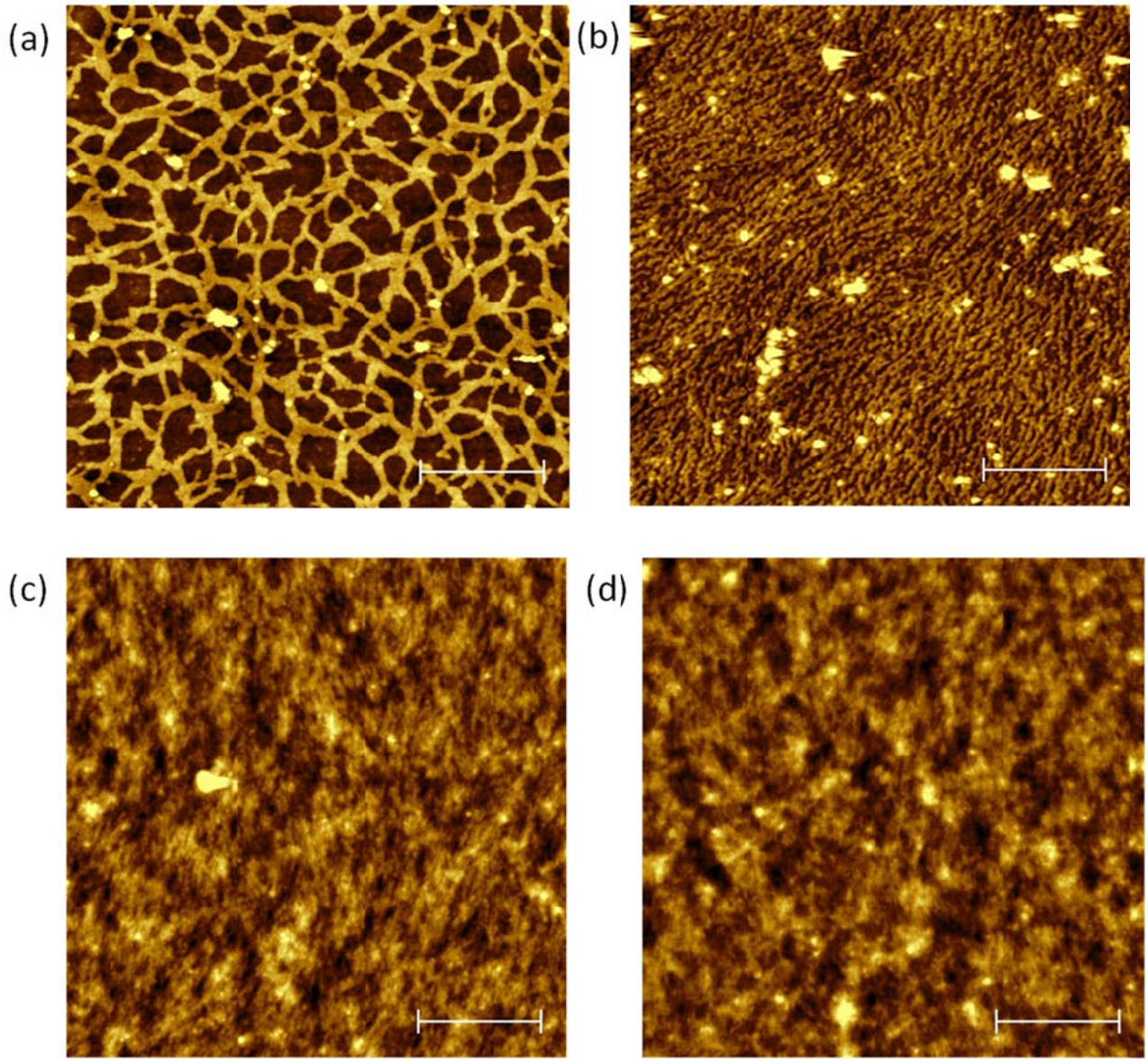


**Figure S11.** AFM height images of PNDIFu2-C20 films spun from toluene at concentration of 0.2 g/L (a), 0.4 g/L (b), 5 g/L (as spun) (c) and 5 g/L (after 30 minutes thermal treatment at 250 °C) (d); dilute solutions reveal the presence of a networked monomolecular (2.5 nm thick) layer in contact with the substrate (a) and the occurring of fibrillar-like morphology with elongated domains mostly aligned along the flow direction already on top of the first layer (b); due to the high roughness ($R_{rms}$ = 0.91 nm) fibrils are hardly distinguishable on top of the thicker films (c,d); high temperature annealing mainly results in more increased surface roughness ($R_{rms}$ = 1.1 nm). In all images, scale bars are 500 nm.

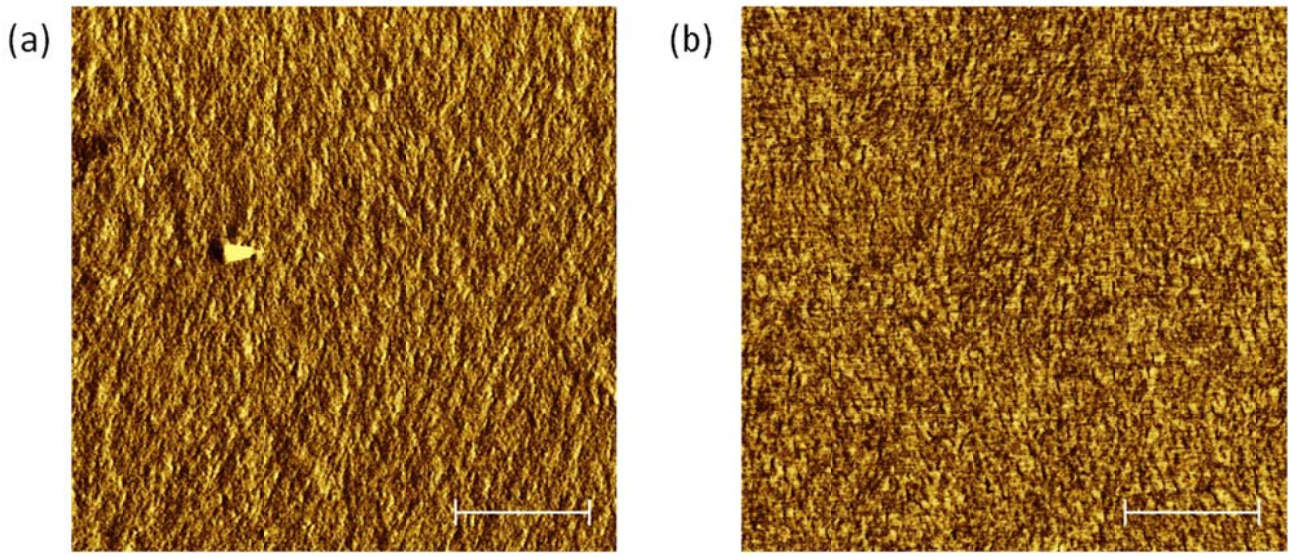


**Figure S12.** AFM phase images of PNDIFu2-C20 films spin coated from 5 g/L solution, as spun (a) and after 250 °C, 30 minutes annealing (b), both suggesting intertwined fibrillar domains still composing the films. In all images, scale bars are 500 nm.

## Computational details

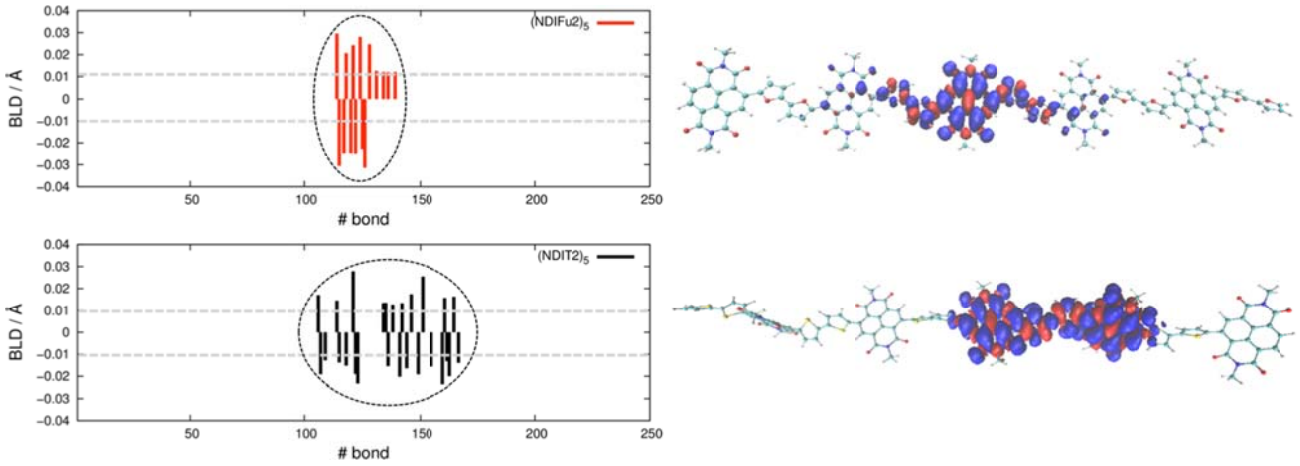


**Figure S13. Left side**: Bond Length Difference (BLD) for $(NDIFu2)_5$ (red bars) and $(NDIT2)_5$. Only those BLD larger than 0.01Å (BLD > 0.01Å) have been reported in order to highlight the different localization of the polaron structural deformations, that is prevalently one polymer unit for the case of $(NDIFu2)_5$ and two units for $(NDIT2)_5$. Right side: polaron spin density distribution for $(NDIFu2)_5$ (up) and $(NDIT2)_5$ (bottom), confirming the localization over one and two polymer units respectively. DFT (ω-B97XD/6-311++G*).

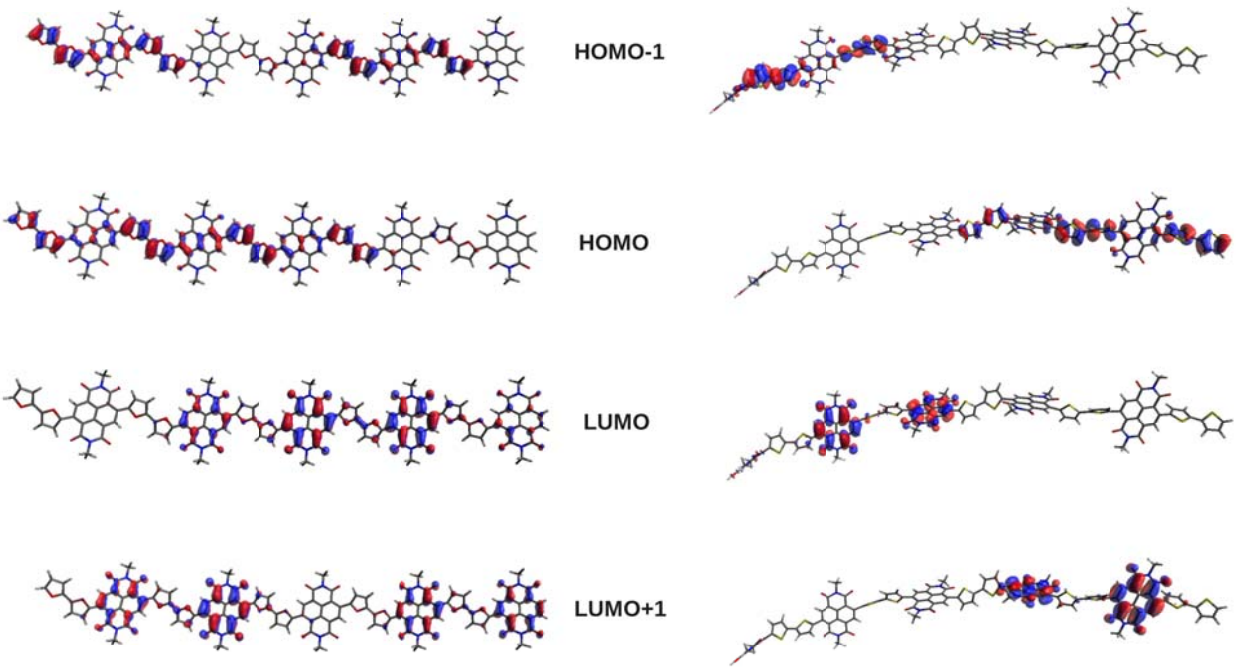


**Figure S14.** Frontier molecular orbital isosurfaces of $(NDIFu2)_5$ and $(NDIT2)_5$ as computed at the ωB97XD/6-311++G* level of theory.

**TDDFT (ωB97XD/6-311++G*) vertical excitations for (NDIFu2)5 in its neutral state.**

**S1 2.3872 eV 519.37 nm f= 5.2086**

*CI composition*
*H -> L (60%)*
*H-1 -> L+1 (20%)*

S2 2.5275 eV 490.55 nm f= 0.0655
S3 2.6630 eV 465.58 nm f= 0.3153
S4 2.7787 eV 446.20 nm f= 0.0071
S5 2.9198 eV 424.63 nm f= 0.0961
S6 3.1066 eV 399.11 nm f= 0.0010
S7 3.1774 eV 390.20 nm f= 0.0032
S8 3.2381 eV 382.89 nm f= 0.0026
S9 3.2777 eV 378.27 nm f= 0.0034
S10 3.7583 eV 329.90 nm f= 0.7808
S11 3.7709 eV 328.79 nm f= 0.0427
S12 3.7744 eV 328.49 nm f= 0.0105
S13 3.7794 eV 328.05 nm f= 0.0540
S14 3.8114 eV 325.30 nm f= 0.3298
S15 3.8416 eV 322.74 nm f= 2.5246

**TDDFT (ωB97XD/6-311++G*) vertical excitations for (NDIT2)5 in its neutral state.**

**S1 2.9496 eV 420.34 nm f= 1.1708**

*CI composition*
*H -> L (50%)*
*H-1 -> L+1 (10%)*

S2 2.9777 eV 416.38 nm f= 0.5770
S3 3.0164 eV 411.04 nm f= 0.0599
S4 3.0522 eV 406.21 nm f= 0.0294
S5 3.1252 eV 396.72 nm f= 0.0002
S6 3.1367 eV 395.27 nm f= 0.0445
S7 3.1603 eV 392.32 nm f= 0.0009
S8 3.1986 eV 387.62 nm f= 0.0028
S9 2.2069 eV 386.61 nm f= 0.0115
S10 3.7939 eV 326.80 nm f= 0.4645
S11 3.8010 eV 326.19 nm f= 0.2772
S12 3.8033 eV 325.99 nm f= 0.4682
S13 3.8073 eV 325.65 nm f= 0.1857
S14 3.8097 eV 325.45 nm f= 0.3549
S15 3.9458 eV 314.22 nm f= 0.6708